NeuroImage 155 (2017) 480–489

Contents lists available at ScienceDirect

NeuroImage

journal homepage: www.elsevier.com/locate/neuroimage

Correspondence between fMRI and electrophysiology during visual motion processing in human MT+☆

Anna Gaglianese[a,b], Mariska J. Vansteensel[a], Ben M. Harvey[c], Serge O. Dumoulin[c,d], Natalia Petridou[b,*,1], Nick F. Ramsey[a,1]

[a] Department of Neurosurgery and Neurology, Brain Center Rudolf Magnus, University Medical Center Utrecht, Utrecht, The Netherlands
[b] Department of Radiology, University Medical Center Utrecht, Utrecht, The Netherlands
[c] Experimental Psychology, Helmholtz Institute, Utrecht University, Utrecht, 3584 CS, The Netherlands
[d] Spinoza Center for Neuroimaging, Amsterdam, The Netherlands

ARTICLE INFO

Keywords:
Electrocorticography (ECoG)
Blood Oxygenation Level Dependent (BOLD)
3 T fMRI
hMT+
Neurovascular coupling
Brain

ABSTRACT

Changes in brain neuronal activity are reflected by hemodynamic responses mapped through Blood Oxygenation Level Dependent (BOLD) functional magnetic resonance imaging (fMRI), a primary tool to measure brain functioning non-invasively. However, the exact relationship between hemodynamics and neuronal function is still a matter of debate. Here, we combine 3 T BOLD fMRI and High Frequency Band (HFB) electrocorticography (ECoG) signals to investigate the relationship between neuronal activity and hemodynamic responses in the human Middle Temporal complex (hMT+), a higher order brain area involved in visual motion processing. We modulated the ECoG HFB and fMRI BOLD responses with a visual stimulus moving at different temporal frequencies, and compared measured BOLD responses to estimated BOLD responses that were predicted from the temporal profile of the HFB power change. We show that BOLD responses under an electrode over hMT+ can be well predicted not only be the strength of the neuronal response but also by the temporal profile of the HFB responses recorded by this electrode. Our results point to a linear relationship between BOLD and neuronal activity in hMT+, extending previous findings on primary cortex to higher order cortex.

Introduction

Since its invention in the early 1990s (Ogawa et al., 1992, 1990), functional magnetic resonance imaging (fMRI) has become a prominent technique to functionally characterize the human brain. FMRI studies are based on task-related or spontaneous changes in the blood-oxygenation-level-dependent (BOLD) signal that is mapped from the venous vasculature. Because blood oxygenation levels and cerebral blood flow change rapidly following changes in the neuronal activity in a brain region (the hemodynamic response), fMRI allows to efficiently, although indirectly, measure brain function non-invasively in humans. It remains unclear, however, how exactly hemodynamics relate to neuronal function in the human brain, and this has become a central issue for the neuroscience community. Invasive animal studies have shown that fMRI signals are highly correlated with neuronal spiking activity as well as with Local Field Potentials (LFPs), which are suggested to reflect input and intracortical processing (Goense et al., 2012; Logothetis et al., 2001; Niessing et al., 2005). Other animal studies have shown, however, that BOLD responses are uncoupled from neuronal activity under certain experimental conditions (Huo et al., 2014; Norup and Lauritzen, 2001; Swettenham et al., 2013). Notably, the relationship observed in animals does not necessarily reflect the characteristics of neurovascular coupling in humans, as observed with fMRI, due to potential differences in cortical anatomy (e.g. cortical folding, Gagnon et al., 2015), vascular anatomy (e.g. vessel geometry, size, and organization, Hirsch et al., 2012; Gagnon et al., 2015), and experimental conditions such as anesthesia (Liu et al., 2013; Pisaro et al., 2013) and task delivery. A limited number of studies have examined the relationship between fMRI and neuronal activity in humans, predominantly using non-invasive electrophysiological modalities such electroencephalography (EEG) or magnetoencephalography (MEG). These studies have shown that spatial maps of fMRI BOLD activity in response to different types of sensory stimulation roughly correspond to EEG and MEG responses in the respective

☆ The authors declare no competing financial interests.

* Correspondence to: Department of Radiology, UMC Utrecht, Heidelberglaan 100, P.O. Box 85500 HP E.01.132, 3584 CX Utrecht, The Netherlands.
E-mail address: N.Petridou@umcutrecht.nl (N. Petridou).

[1] Co-authorship.

http://dx.doi.org/10.1016/j.neuroimage.2017.04.007
Received 23 November 2016; Received in revised form 7 March 2017; Accepted 3 April 2017
Available online 05 April 2017

primary sensory cortices (Brookes et al., 2005; Im et al., 2007; Mukamel et al., 2005; Rosa et al., 2010; Singh et al., 2002). However, since the spatial resolution of EEG and MEG is lower than that of fMRI measurements, it is difficult to establish a one-to-one relationship between neuronal and BOLD signals.

Intracranial electrocorticography (ECoG), has recently received increasing attention due to its unique combination of high spatial and temporal resolution. ECoG allows direct measurement of electrical activity in neuronal populations covering a few millimeters of gray matter, directly underneath the electrode. The spatial resolution afforded is high, similar to that of fMRI measurements, which facilitates direct comparison between the two modalities in the same patch of cortex. Although ECoG is typically acquired in epilepsy patients, studies have shown that measurements acquired from non-epileptic tissue yield results that are considered normal in terms of expected location and functional response to tasks (Jacobs et al., 2010). Furthermore, ECoG provides separable measurements of not only neural oscillatory activity but also of changes in high frequency broadband (HFB) power, which is associated with spiking activity (Miller et al., 2009), with very high sensitivity, although high frequencies may also be detected with high density EEG (Onton and Makeig, 2009). Combined ECoG-fMRI studies have recently provided evidence of a direct spatial correlation of BOLD responses with HFB power (Mukamel et al., 2005; Hermes et al., 2012; Siero et al., 2013; Jacques et al., 2016). However, several factors complicate the comparison of BOLD responses and neuronal responses measured by ECoG. First, studies have tended to focus on spatial correlation. Spatial correlation alone does not allow for assessment of the exact relationship between the measured fMRI signal and the underlying neuronal activity, leaving open the question of linearity of this relationship in neurovascular coupling. Second, BOLD responses are usually modeled following experimental design such as stimulus timing, rather than using the temporal profile of neuronal responses. This may be a suboptimal approach, as a recent combined 7 T fMRI-ECoG study showed that the exact neuronal responses can predict BOLD responses more accurately than a model based on stimulus timing, in the case of increasing frequency of movement in motor cortex (Siero et al., 2013). Third, the relationship between fMRI activity and neurophysiological recordings has predominantly been studied in primary sensory and motor cortices, while much of human brain consists of higher order regions of the cortex where stimuli cannot readily be controlled.

The present study was conceived to determine the linearity of neurovascular coupling in higher order cortex. We focused on the human Middle Temporal complex (hMT+), a higher order brain area involved in visual motion processing (Amano et al., 2009; Dumoulin et al., 2000; Huk et al., 2002; Tootell et al., 1995). We modulated the ECoG and fMRI BOLD responses by engaging subjects in a visual task consisting of a moving, high contrast, black and white dartboard, the contrast of which was reversed at different temporal frequencies. This type of stimulus is known to elicit strong activity in hMT+ in both modalities (Gaglianese et al., 2015; Harvey et al., 2013; Kastner et al., 2003; Winawer et al., 2013) and to generate distinct and independent responses in HFB power for each of the spatial and temporal frequencies of the visual stimuli, as measured with ECoG (Gaglianese et al., 2016). We used these HFB power changes to predict the related BOLD responses and compared the predicted responses with real, measured BOLD responses for the same task and the same subjects using 3 T fMRI. We show a close correspondence between the predicted and measured hemodynamic response functions (HRF) and conclude that there is a linear relationship between the hemodynamic responses in hMT+ and both the amplitude and the temporal profile of the underlying neuronal activity.

Materials and methods

Subjects (three males, one female) were epilepsy patients who underwent implantation of subdural electrode grids to determine the site of epileptic foci for the purpose of possible surgical removal of the epileptogenic tissue. Implanted grids extended to healthy tissue in the hMT+ area of the left (n=2) and right (n=2) hemisphere. Before the subdural electrode implantation, subjects underwent an fMRI scan and were presented with visual motion stimuli identical to the ones performed during ECoG measurements, except that the presentation timing was adjusted to match the timing of the hemodynamic (fMRI) responses. A high resolution (0.5×0.5×1 mm) 3D computed tomography (CT, Philips TomoscanSR7000) scan was acquired after implantation to localize ECoG grid electrodes on each subject's brain. The study was approved by the medical ethical board of the Utrecht University Medical Center. All subjects gave their written informed consent to participate in the study in compliance with the Declaration of Helsinki 2013.

fMRI

fMRI data were acquired on a Philips Achieva 3 T scanner using 3D PRESTO (Neggers et al., 2008; Ramsey et al., 1996; van Gelderen et al., 2012) and a commercial 8-channel head coil. For one subject, 40 slices were acquired with a field of view (FOV) of 224×256×160 mm, resulting in a voxel size of 4 mm isotropic. Functional volumes were acquired every 608 ms with a flip angle of 10 degrees, echo time (TE) of 33.2 ms, and repetition time (TR) of 22.5ms. For the other three subjects the FOV was 99×256×182 mm for a total of 33 slices encompassing the visual cortex and posterior temporal lobes, and voxel size 3mm isotropic. Functional volumes were acquired every 810 ms with flip angle of 10 degrees, TE of 38.7 ms and TR of 27 ms. At the beginning of each experimental session, whole-brain gradient-echo T1-weighted images were acquired at a resolution of 1 mm isotropic, for all subjects.

fMRI stimuli

Subjects were presented with a visual stimulus that consisted of a high-contrast black-and-white dartboard with a fundamental spatial frequency of 0.33 cycle/deg. During the motion-on condition, visual motion covering the entire display was shown for 1 s and the dartboard expanded with a fundamental temporal frequency of 1, 3 or 5 Hz in different trials. Each temporal frequency was presented 27 times in a single run, for a total of three runs. Outside of these motion periods, a stationary black-and-white dartboard with spatial frequency of 0.33 cycle/deg was presented. The interval between motion periods was based on equal distribution of inter-stimulus-intervals (ISI) ranging between 6 s and 15 s (2 trials per ISI, in 1 s increments), plus 6 trials with 19 s and 24 s ISI (3 each). The order of ISIs was pseudo-randomized, and the same order was used for each run. Due to timing constraints, two subjects were able to perform only two runs (1 and 5 Hz condition respectively). Visual stimuli were back-projected on a 24 in. display with 1920×1200 pixel resolution inside the MRI bore. Subjects viewed the display through a mirror with a total distance from the subject's eyes to the display screen of 90 cm. The scanner room was kept dark. To ensure subjects attended to the stimulus and maintained accurate fixation, subjects were instructed to perform a color change detection task on the fixation dot in the middle of the display, where a button press was required for every color change of the fixation dot.

fMRI analysis

For each subject, cortical surface estimation was computed by automatically segmenting the T1-weighted anatomical scan using FreeSurfer (http://surfer.nmr.mgh.harvard.edu). Gray matter volumes were then rendered as a smoothed 3D cortical surface.

Functional data were pre-processed using AFNI (http://afni.nimh.nih.gov/afni, Cox 1996). All datasets underwent rigid-body motion correction, temporal linear detrending, and alignment of functional and anatomical data. No spatial smoothing was applied.

hMT+ localization. For each subject, the location of hMT+ was identified with multiple regression analysis. The fMRI runs were concatenated, and the analysis was performed by contrasting the responses of moving (all temporal frequencies combined) versus stationary dartboards (using the 3dDeconvolve function in AFNI), obtained by convolution of the task with a standard hemodynamic response model (Boynton et al., 1996). The resulting activation map was used to identify the ECoG electrode on hMT+ (see ECoG-fMRI co-localization section). The 6 movement parameters derived from the motion correction (3 translation, 3 rotation) were included as regressors of no interest. Activation maps were visualized on each subject's rendered brain surface using the SUrface MApping (SUMA) software in AFNI.

hMT+ responses to different temporal frequencies. Data from each functional scan consisted of 27 trials of a single temporal frequency condition. The mean hemodynamic response function (HRF) for each temporal frequency (1, 3 or 5 Hz), that is, each motion stimulus condition, was reconstructed for all voxels in the volume imaged using a deconvolution approach (Dale, 1999). This method does not infer any a priori model of the HRF response, except for the duration of the HRF, which was set to 25 s in accordance with previous studies (Costagli et al., 2014; Gaglianese et al., 2015; Gardner et al., 2005). This type of analysis also provides an r^2 and significance value. Significantly activated voxels for each motion stimulus condition were based on statistics on the r^2 values obtained by a bootstrapping procedure using a permutation analysis method (Gardner et al., 2005). In short, the r^2 values were recomputed 100 times for each voxel using a randomized version of the stimulus timing presentation to obtain a single distribution of r^2 values representing the distribution expected by chance. An r^2 value at cut-off p-value=0.05 was compared to the r^2 value of each voxel in order to detect significant voxels. The analysis was performed using mrTool (http://gru.stanford.edu/doku.php/shared/home).

ECoG

Implanted grid electrodes had a measurement surface of 2.3 mm diameter per electrode, with 1 cm inter-electrode spacing, and were positioned directly on the cortical surface. A reference electrode was positioned extra-cranially on the mastoid bone. The recording system was a 128 channel Micromed system (Treviso, Italy). Data were acquired with a sampling rate of 512 Hz and band-pass filtered between 0.15–134.4 Hz.

ECoG Stimuli

During the ECoG experiment, subjects performed one run, in which the same visual stimuli as used in the fMRI measurements were presented. Because of the high temporal resolution of the ECoG recordings, all temporal frequencies could be presented in a single run, with random inter-stimulus intervals ranging between 3 s and 4.5 s. Each temporal frequency was shown 18 times. For one subject, temporal frequencies (1 Hz and 5 Hz) were presented in two different runs. The visual stimulus properties and the room setup were adjusted to be identical to the ones used in the fMRI scans. Stimuli were presented in a dark room using a Toshiba Tecra S10-101 laptop (Toshiba, Tokyo, Japan) and displayed on a 1024×768 pixel LCD screen (Samsung Syncmaster 214 T, Seoul, Korea) positioned in front of the patient at a distance of 75 cm from the eyes. Subjects performed the same color change detection task as in the fMRI session.

ECoG analysis

ECoG signal quality was inspected by a neurologist and electrodes with large epileptic artefacts, flat signal or excessive noise were rejected. The remaining electrodes were re-referenced to the common average of all remaining electrodes. For each electrode and stimulus motion condition, data were filtered in the HFB (65–95 Hz), alpha (8–14 Hz) and beta (15–25 Hz) bands using a third-order Butterworth filter in two directions to minimize phase distortion (using the filtfilt function in MATLAB; MathWorks). Then, the smoothed log power of the analytic amplitude by Hilbert transform was calculated (Hermes et al., 2012). For each temporal frequency condition, motion stimulus related epochs were defined as the 1 s periods of motion presentation. Baseline epochs started 1 s after motion offset and lasted 1 s. Mean responses across the 18 motion stimulus epochs for each temporal frequency condition were computed for each frequency band and the mean of the baseline epochs was subtracted. Finally, the responses were converted to z-scores by dividing by the standard deviation of the mean baseline epoch. In addition, only in the case of the HFB band, we summarized responses across subjects and temporal frequencies by extracting the area under the corresponding HFB z-score response profile during the 1 s of motion plus 500ms to allow the power increase to return to baseline.

The spectrogram for all temporal frequency conditions was also computed using a multi-taper spectrum function and a moving window with time-width of 0.5 s and step size 50ms, as implemented in Chronux (chronux.org).

ECoG-fMRI co-localization

Implanted electrodes were automatically localized on the post-operative high resolution CT scan using the 3Dclustering detection function provided by AFNI (Branco et al., 2016). The CT was co-registered and re-sliced to the T1-weighted anatomical scan using normalized mutual information (Wells et al., 1996). After co-registration, electrode coordinates were corrected for the brain shift caused by the surgery (Hermes et al., 2010), then projected onto the nearest cortical surface point in the anatomical MRI. A single ECoG electrode on hMT+ was identified for each subject, based on the proximity to the significant active voxels obtained by the fMRI activation map that resulted from the multi regression fMRI analysis ($p < 0.05$). The location of the identified electrode on hMT+ was confirmed anatomically for each subject (the intersection of the junction between the ascending limb of the inferior temporal sulcus and the sulcus itself (Dumoulin et al., 2000)). For data matching, fMRI voxels were selected within a radius of 8mm from the center of mass of the selected electrode based on previous work (Hermes et al., 2012), provided they were significant according to the deconvolution analysis, (r2-value $P < 0.05$), and the time courses were averaged to a single fMRI measure.

ECoG-fMRI modeling

We modeled BOLD responses to each visual motion condition based on the temporal profile of the ECoG spectral responses (Fig. 1). ECoG-based BOLD responses were constructed as follows: First, z-scored spectral power changes in HFB were computed for each electrode and temporal frequency condition, as described in the ECoG analysis section. Second, ECoG-based time-series were simulated by multiplying the mean z-scored responses for each temporal frequency with a boxcar function with duration of 1.5 s and amplitude 1, interleaved by the inter stimulus trial interval used in the fMRI experiment (Fig. 2A). The time resolution of the entire simulation was set to 50 ms. Third, the derived ECoG-based time-series were convolved with a HRF based on a gamma function (Boynton et al., 1996), giving a prediction of the fMRI time-series. The simulated fMRI time-series were normalized to zero mean and unit variance and were sampled every TR step to match the timing of the signal acquisition by the scanner (Fig. 2, B-C). The estimated ECoG-$BOLD_{HFB}$ was finally computed for each temporal frequency condition by deconvolution of

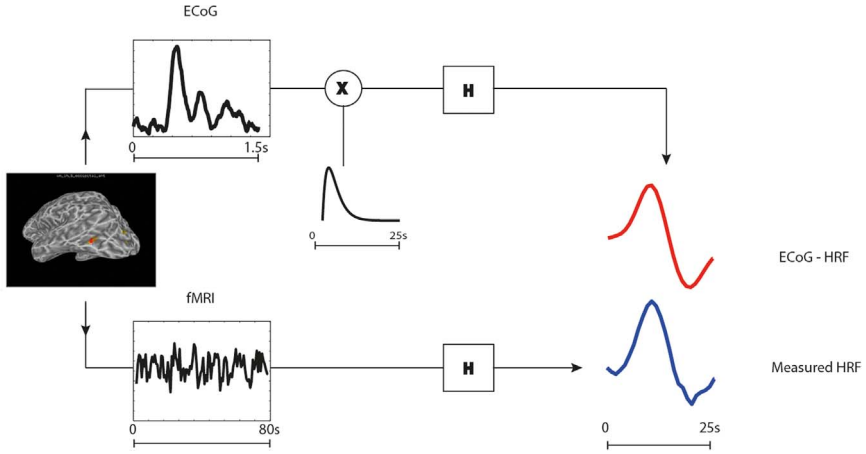

Fig. 1. ECoG-fMRI modeling and experimental protocol. We recorded neuronal and hemodynamic responses to visual motion stimuli using both ECoG (top left) and fMRI (bottom left) measurements from the hMT+ complex of each subject. The measured HRF (blue curve) was estimated by deconvolution of the fMRI BOLD time series (bottom row). It was compared to the modeled ECoG HRF (red curve), which was obtained by convolving the ECoG spectral power changes in the high frequency band with a gamma function (top row).

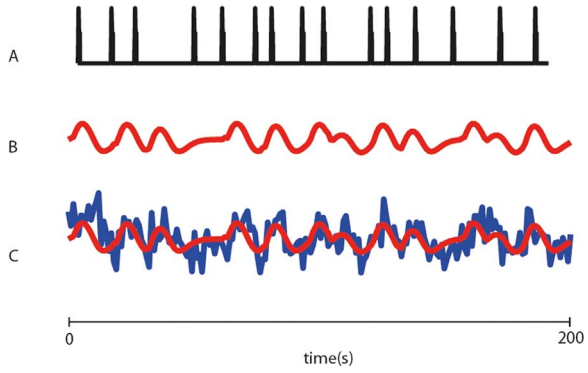

Fig. 2. ECoG HFB power spectral changes predict the BOLD fMRI time series with high accuracy. A) HFB responses to repetitive presentation of the same 1 s visual motion stimulation. B) Estimated ECoG-fMRI time series computed by convolving the ECoG time-series (A) with a standard gamma hemodynamic response function and resampled to the fMRI volume acquisition time. C) Measured fMRI time series (blue) to the same visual motion stimulation of (A) superimposed by the fMRI time series predicted from the ECoG response shown in (B) (red). The fMRI time series predicted from the ECoG responses is consistent with the measured fMRI time series.

each simulated ECoG-based fMRI time-series. The same procedure was followed using ECoG responses in the alpha and beta band to estimate ECoG-BOLD$_{alpha}$ and ECoG-BOLD$_{beta}$ respectively.

Finally, the measured-BOLD responses for the three temporal frequency conditions were computed for each resultant time-series by deconvolution (see fMRI analysis section).

ECoG-BOLD vs measured-BOLD responses

To determine whether the estimated ECoG-BOLD responses predicted the measured-BOLD, we first computed for each subject and each temporal frequency condition the goodness of fit by the root mean square error (RMS) between the predicted ECoG-BOLD and measured-BOLD response. We then quantified the response to each motion stimulus by extracting the amplitude and the area under the curve of each corresponding ECoG-BOLD and measured-BOLD response. Similarity across subjects and temporal frequency conditions was quantified by correlating ECOG-BOLD and measured-BOLD amplitudes and areas under the curve across subjects and temporal frequency conditions. To test whether alpha and beta frequency bands explained additional variance in the BOLD responses, independently of HFB changes, we computed the partial correlation between the measured-BOLD and estimated ECoG-BOLD$_{HFB}$ amplitudes and areas, controlling for ECoG-BOLD$_{alpha}$ and ECoG-BOLD$_{beta}$ values.

Results

FMRI and ECoG activation in hMT+

During visual motion presentation, subjects consistently exhibited positive BOLD responses in the human MT complex (hMT+) and early visual cortex (Fig. 3). Only the responses in hMT+ were used for further analysis.

The ECoG measurement from the electrode located on hMT+ of each subject exhibited a significant spectral power increase in the HFB band ($p < 0.05$, Bonferroni corrected) during visual motion presentation. This spectral increase was within hMT+, as confirmed by the spatial overlap of the ECoG electrode and the fMRI activation foci (Fig. 3).

ECOG and fMRI responses to different temporal frequencies of the visual stimuli

Fig. 4 shows the spectral power in frequencies across the 1–100 Hz range, from stimulus onset (t(0)) to 1 second thereafter, for the three temporal frequency conditions combined. Each temporal frequency elicited significant ECoG HFB and BOLD responses in hMT+ (Fig. 5). Interestingly, ECoG (Fig. 5, left columns) and fMRI responses (Fig. 5, right columns) showed a similar pattern of amplitude responses to the different temporal frequencies, per subject, although differences were observed between subjects. Moreover, the area under the HFB z-scored responses was significantly correlated with the maximum amplitude values of each corresponding measured BOLD response ($r=0.74$, $p=0.015$).

Linear correspondence between measured-BOLD and predicted ECoG-BOLD$_{HFB}$ responses

In order to investigate the relationship between neurophysiological activity and BOLD responses, we predicted the BOLD responses for each motion stimulus condition based on ECoG spectral power changes in HFB, as well as in alpha and beta bands. Root mean square (RMS) between the two curves indicated a good match between measured and ECoG$_{HFB}$ based BOLD responses (Fig. 6).

We summarized the pattern of responses across subjects and temporal frequency conditions by computing the amplitudes and areas of each measured-BOLD and ECoG-BOLD$_{HFB}$. ECoG-BOLD$_{HFB}$ amplitudes were found to be significantly correlated with measured-BOLD amplitudes ($r = .85$, $p < 0.001$, Fig. 7A). Positive correlations indicate that a positive increase in HFB corresponds to a positive increase in

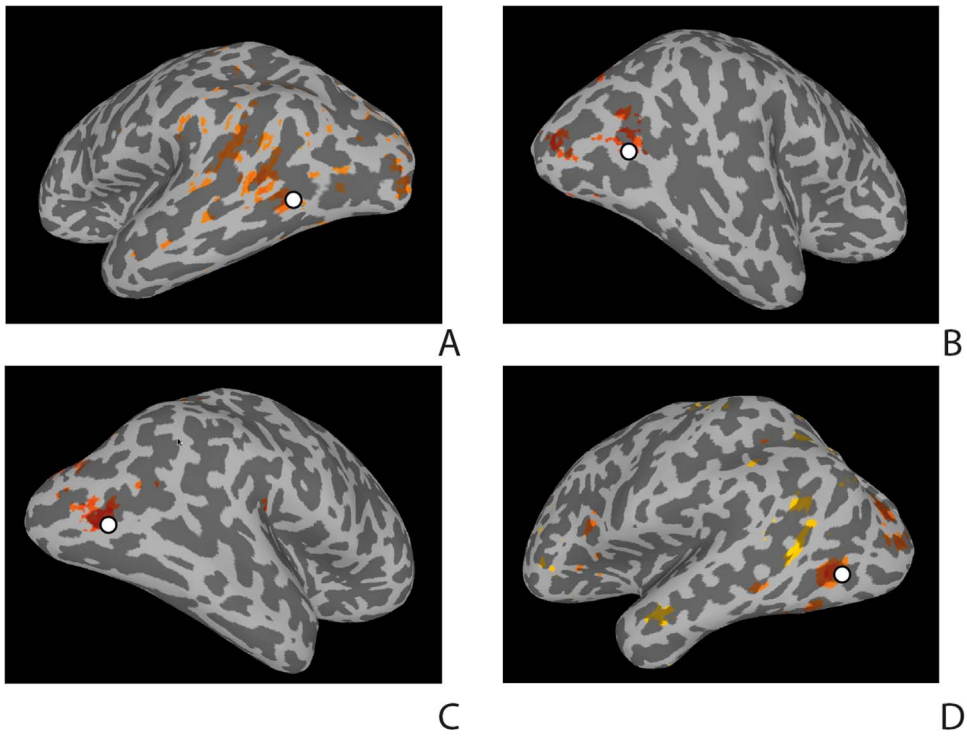

Fig. 3. Visualization of fMRI activation maps for motion compared to stationary stimuli ($p < 0.01$, FDR corrected), together with the location of the ECoG electrode on hMT+ (white dots) for each subject's 3D rendered brain.

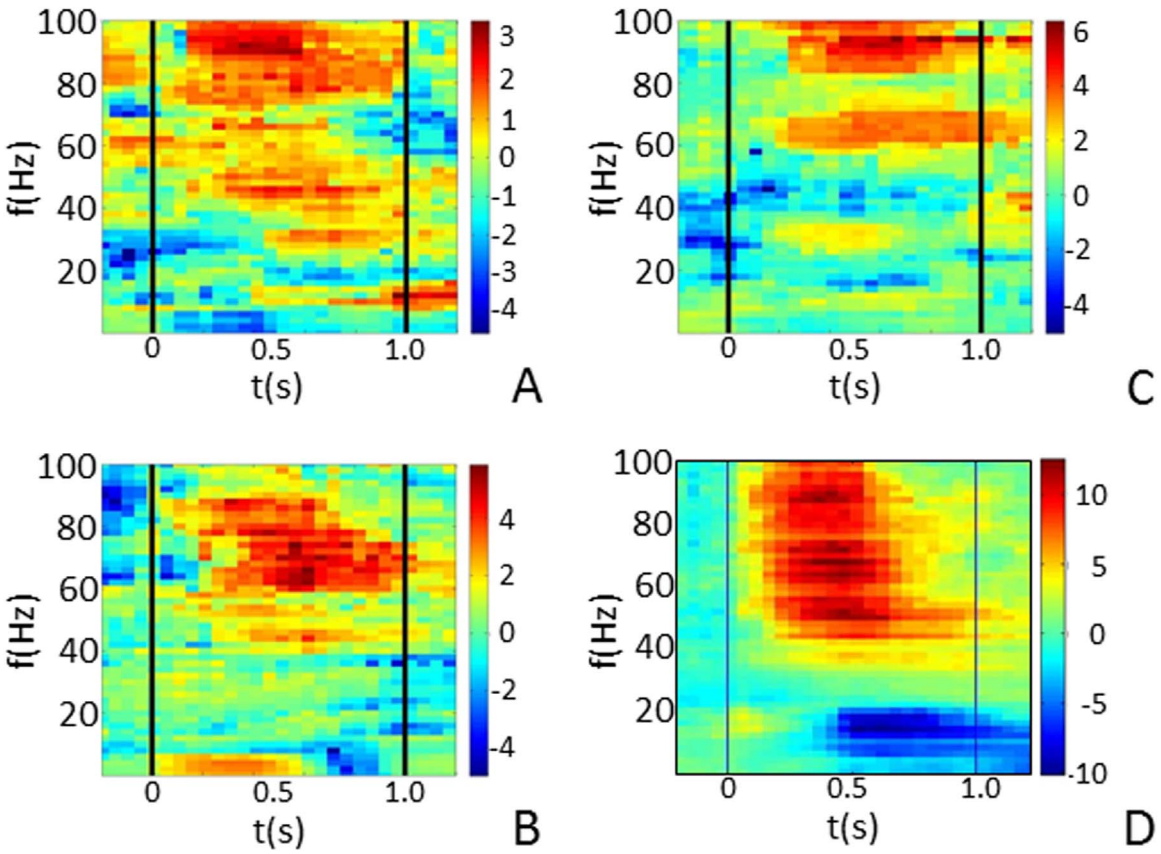

Fig. 4. Figures display the evolution of power in frequencies across the 1–100 Hz range, from stimulus onset (t(0)) to 1 second thereafter, marked by vertical black lines, for the three temporal frequency conditions combined. Color represents the power over time. The data were obtained using a multi-taper spectrum function and a moving window with time-width 0.5 sec and step size 50ms, as implemented in Chronux. Panels A-D show results for each of the 4 subjects.

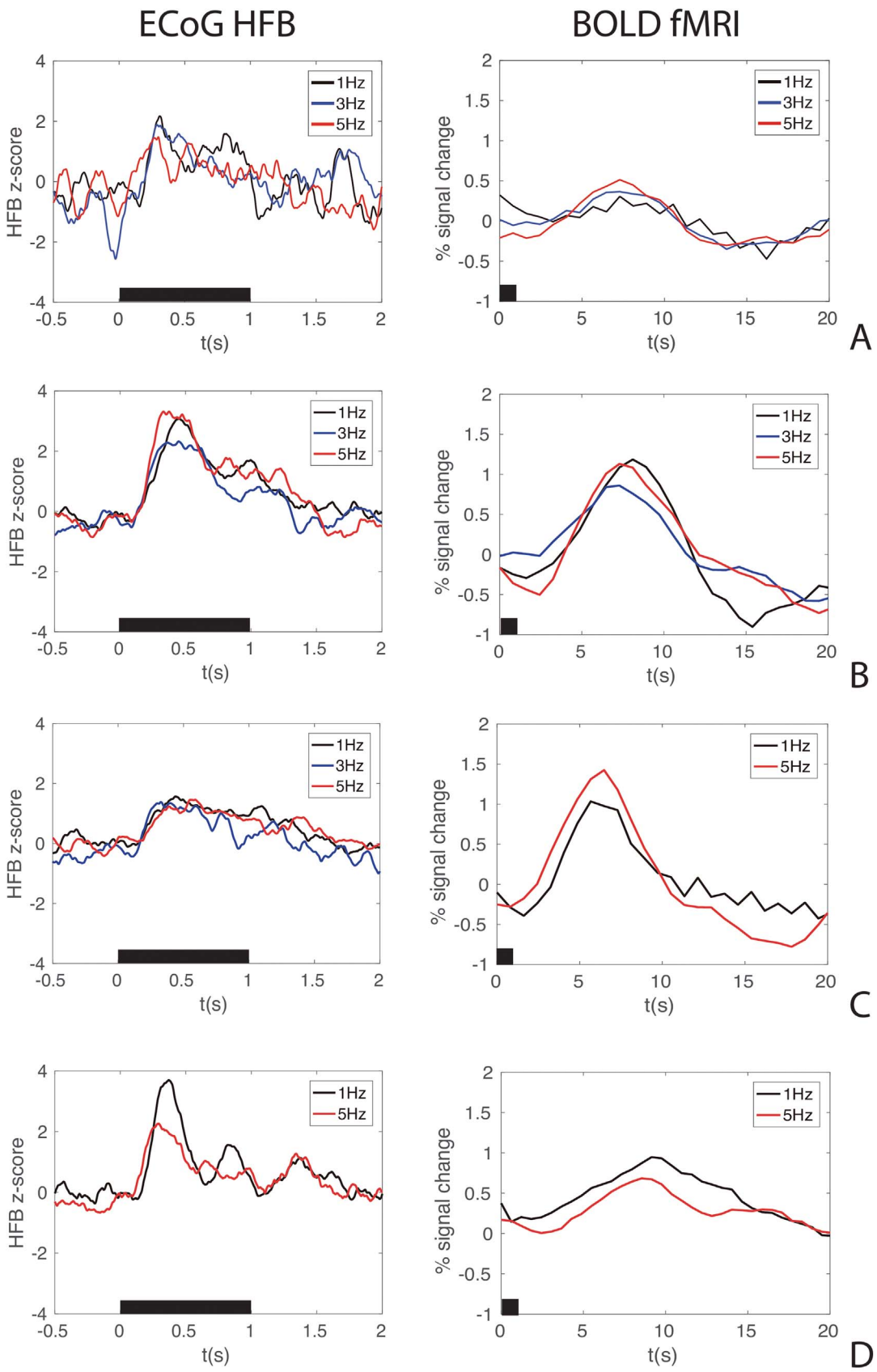

Fig. 5. Rows A to D show the data for subject 1 to 4 respectively. Left columns: mean ECoG HFB responses over trials in hMT+ to 1 s visual motion stimuli of various temporal frequencies, starting at 0 s (black bar represents the stimulus presentation time). Right columns: Mean BOLD responses over trials, measured underneath the ECoG electrode in hMT+, to the same visual motion stimuli (black bar represents the stimulus presentation time).

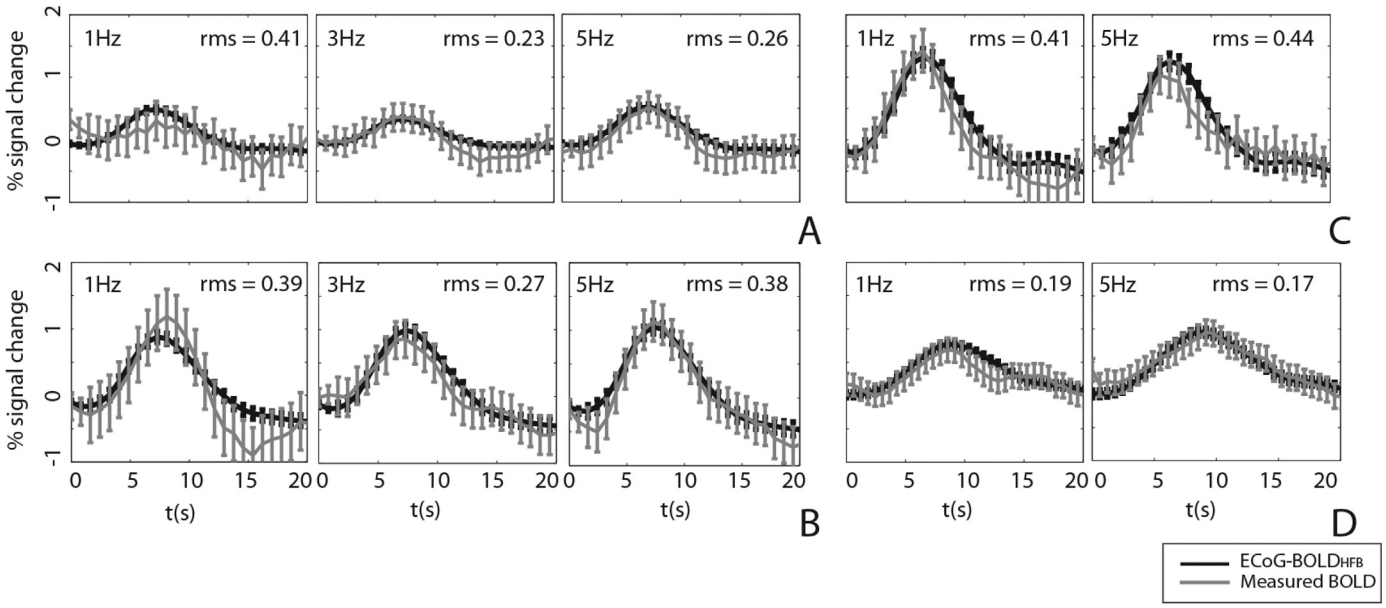

Fig. 6. ECoG power increases in the high frequency band predict measured BOLD responses well. Each panel shows, for each subject (A-D represent individual subjects) and temporal frequency, the mean across trials (± standard error) of the BOLD response predicted from the ECoG response (ECoG-$BOLD_{HFB,}$ black curve), and the measured-BOLD (gray curve).

BOLD responses. Even stronger positive correlations were found between ECoG-$BOLD_{HFB}$ area values and measured-BOLD area values ($r = .95$, $p < 0.001$, Fig. 7B). Interestingly, the strong positive correlation between ECoG-$BOLD_{HFB}$ responses and measured-BOLD response seems to be driven primarily by differences between subjects.

ECoG-$BOLD_{alpha}$ and ECoG-$BOLD_{beta}$ do not explain additional variation in the BOLD responses

To examine whether including low frequency ECoG rhythms together with the HFB responses results in a better prediction of the measured BOLD responses, we computed, for both amplitude and area values, the correlations between measured-BOLD and ECoG-$BOLD_{HFB}$ values supplemented with the ECoG-$BOLD_{alpha}$ and ECoG-$BOLD_{beta}$ responses either separately, or combined. We found that for both amplitudes and areas, the addition of low frequencies did not add any statistical significance increment in terms of explained variance (one-sided t-test, $p < 0.05$), and that HFB is the most informative band in order to predict the measured-BOLD responses (Fig. 8).

Discussion

In the present work, we measured fMRI and ECoG responses in the same subjects to determine whether changes in neuronal activity due to different, carefully controlled, stimulus properties were directly reflected in the BOLD fMRI responses in the higher order visual cortex region hMT+. We show that we were able to predict with high accuracy (correlation r=0.95) the BOLD responses using the temporal profile of ECOG HFB responses. Our results point to a linear relationship between BOLD and neuronal activity in hMT+, extending previous findings on primary cortex to higher order cortex.

hMT+ responses to different temporal frequency of visual stimulation match across ECoG HFB and fMRI BOLD measurements

Our data show that the neuronal responses in hMT+ to different visual motion stimuli, as measured with ECoG, correspond to those measured with fMRI in the same subjects. With both methods, we found that, during the motion-on condition, subjects consistently exhibited positive BOLD and HFB power augmentation within hMT+ in response to the different temporal frequencies of the visual motion

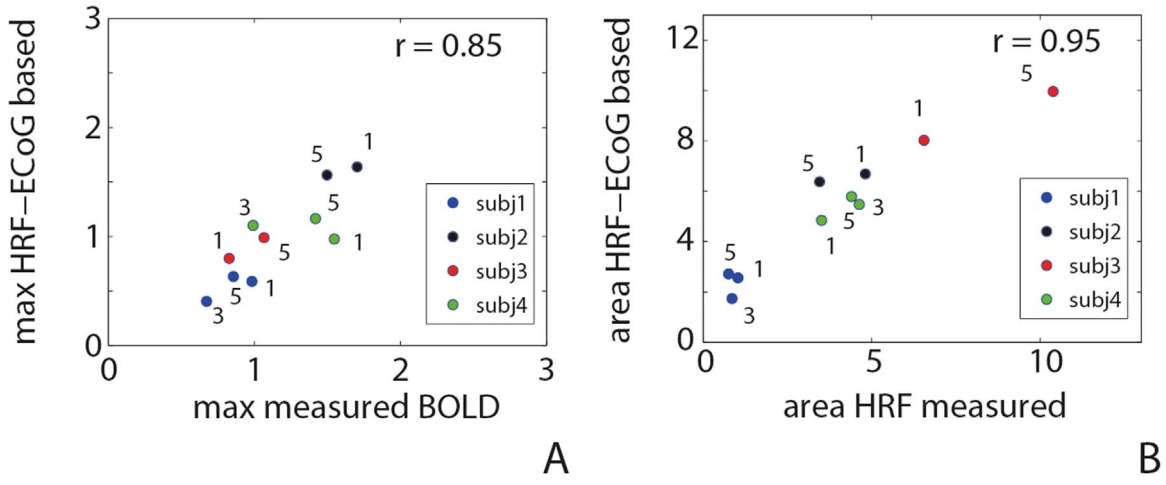

Fig. 7. Correspondence between ECoG-$BOLD_{HFB}$ and measured BOLD summarized across subjects (color coded) and 1, 3 and 5 Hz temporal frequencies (labeled as 1, 3 and 5 respectively). A) Correlation between ECoG-$BOLD_{HFB}$ and measured BOLD *amplitude* values. B) Correlation between ECoG-$BOLD_{HFB}$ and measured BOLD *area* values.

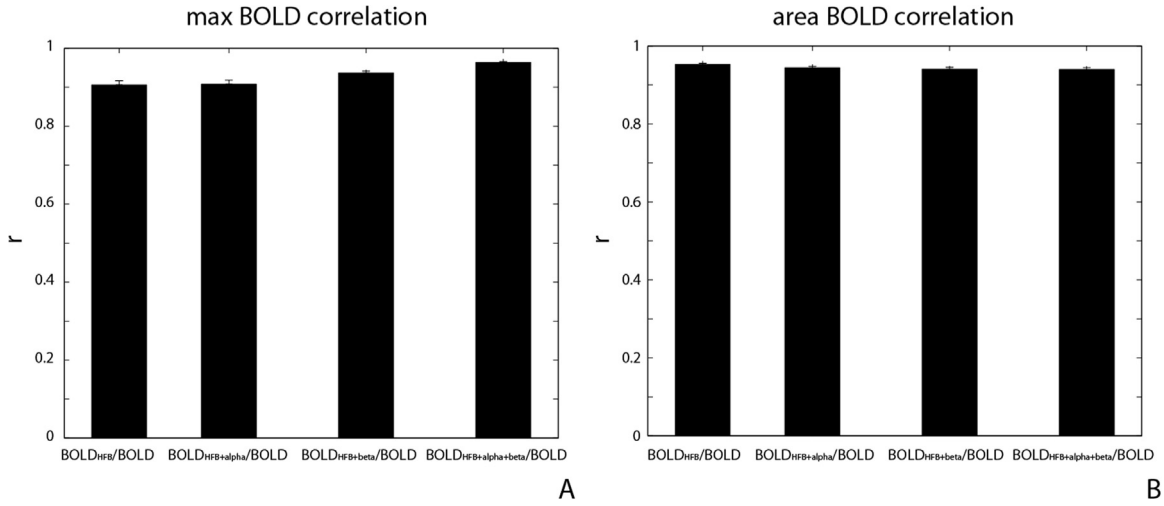

Fig. 8. A) Partial correlation coefficients r2 between ECoG-$BOLD_{HFB}$ and measured-BOLD amplitudes (A) and area (B) values considering values, considering, besides ECoG-$BOLD_{HFB}$, also ECoG-$BOLD_{alpha}$, ECoG-$BOLD_{beta}$ and both ECoG-$BOLD_{alpha}$ and ECoG-$BOLD_{beta}$ as regressors.

stimuli. Our measurements show a nonlinear correspondence between the temporal frequencies of the visual stimuli presented and the amplitudes and area under the curves values of the BOLD as well as the HFB responses. These results are in agreement with previous data from our group (Gaglianese et al. 2016) and other research groups (Chawla et al., 1998; Lui et al., 2007). Our data extend these prior studies, which examined hMT+ responses either with ECoG or with fMRI, by providing evidence of similar amplitude values to the different temporal frequencies between neuronal and BOLD responses measured in the same location. This result suggests a tight relationship between the local synaptic activity in hMT+ and the peak of the concurrent hemodynamic response. This is in agreement with (Hermes et al., 2012; Jacques et al., 2016; Mukamel et al., 2005; Niessing et al., 2005) and in particular with (Magri et al., 2012), who showed that amplitude variations of the BOLD signal reliably followed increases and decreases in gamma power.

ECoG HFB responses accurately predict measured BOLD responses

To quantify the correspondence between ECoG-HFB and BOLD, we used the temporal profiles of the ECoG HFB power responses to predict the corresponding BOLD responses, and compared the resulting predicted BOLD responses with measured BOLD responses, acquired in the same location. Results show that BOLD activity under an electrode over hMT+ can be well predicted by the temporal profile of the HFB responses recorded by this electrode. In particular, BOLD amplitudes and area values predicted from the profile of the HFB responses during the motion-on condition were tightly correlated with both the amplitudes and the area of the measured BOLD responses, suggesting a linear relationship with not only the strength of the neuronal response (represented by the peak of the predicted and measured BOLD responses) but also with the temporal profile of neuronal activity (described by the correspondence between the areas under the predicted and measured BOLD responses), which represents the energy needed by the neural activity to respond to the task.

The present study extends previous findings of combined ECoG-fMRI studies, which report a spatial correlation of BOLD responses with HFB power (Hermes et al., 2012; Jacques et al., 2016; Miller et al., 2009; Mukamel et al., 2005; Siero et al., 2013), providing evidence of an additional agreement in temporal features. Moreover, linearity between hemodynamics and neuronal responses has also been confirmed by a previous combined 7 T fMRI-ECoG study on primary motor and somatosensory cortex that showed that HFB power responses predict the BOLD responses more accurately than stimulus timing alone (Siero et al., 2013). Our findings demonstrate that this linear correspondence between neuronal activity and BOLD remains valid also for 3 T measurements, corroborating the reliability of 3 T BOLD fMRI studies to study brain functioning.

Finally, although more experimental stimuli conditions, such as varying the duration of the stimulation, are needed, our findings suggest that apparent non linearity between BOLD and neuronal activity in other cortical regions and with different sensory stimuli (Magri et al., 2011; Norup and Lauritzen, 2001; Swettenham et al., 2013) might originate by non-linearity of the neuronal responses rather than non-linearity in the vascular in response to neuronal events.

Neuronal responses may contribute to inter-subject variability of BOLD responses

Interestingly, as shown in Fig. 7, the close correspondence between BOLD responses predicted by the ECoG HFB responses and measured BOLD responses is also driven by differences between subjects. It is possible that these differences may be due to (slight) different electrode location across subjects within hMT+ that may lead to different neuronal and BOLD responses within the complex. Other factors such as age of the patients and performance may also be reflected in the neurovascular responses measured. Alternatively, this result may suggest that differences in BOLD response between subjects reflect differences in neuronal response amplitudes and temporal profiles, which could be a contributing factor to the inter-subject variability observed in fMRI studies. This would be in line with the observation that the neurovascular response is subject-specific in monkey visual cortex (Logothetis et al., 2001). It has been reported that regional variations in vascular density can relate to regional variations in BOLD amplitude (Vigneau-Roy et al., 2014) which could also explain the differences in the BOLD response between subjects. However, variations in vascular density alone are not likely the source of the close correspondence between the BOLD responses predicted by the ECoG HFB responses and the measured BOLD responses observed here across subjects. It has been shown that vascular density correlates with cellular density and expected metabolic demand (Adams et al., 2015, Blinder et al., 2013, Bell and Ball 1985, Weber et al., 2008) which could be a neurovascular coupling mechanism that can explain the linear relationship between the measured and ECoG-HFB predicted BOLD. More subjects, however, are needed to investigate the source of response differences between subjects.

In summary, we have shown that ECoG HFB responses in hMT+ explain the variance of the measured BOLD response in this area, and conclude that BOLD fMRI measures can accurately estimate the

underlying neuronal electrophysiological response to stimuli not only in primary but also in higher order cortex.

Acknowledgments

This work was supported by the Netherlands Organization for Scientific Research (NWO), Vidi Grant number 13339 (N.P.), the European Research Council (ERC) Advanced 'iConnect' project, number 320708 (N.F.R.), and the National Institute of Mental Health of the National Institutes of Health under award number R01MH111417. The authors would like to thank Erik J. Aarnoutse, Frans S.S. Leijten, Cyrille H. Ferrier, Tineke Gebbink and all the clinical neurophysiology team for the experimental environment and their help in collecting the data.

References

Adams, D.L., Piserchia, V., Economides, J.R., Horton, J.C., 2015. Vascular supply of the cerebral cortex is specialized for cell layers but not columns. Cereb. Cortex 25, 3673–3681.

Amano, K., Wandell, B.A., Dumoulin, S.O., 2009. Visual field maps, population receptive field sizes, and visual field coverage in the human MT+ complex. J. Neurophysiol. 102, 2704–2718. http://dx.doi.org/10.1152/jn.00102.2009.

Bell, M.A., Ball, M.J., 1985. Laminar variation in the microvascular architecture of normal human visual cortex (area 17). Brain Res. 335, 139–143.

Blinder, P., Tsai, P.S., Kaufhold, J.P., Knutsen, P.M., Suhl, H., Kleinfeld, D., 2013. The cortical angiome: an interconnected vascular network with noncolumnar patterns of blood flow. Nat. Neurosci. 16, 889–897.

Boynton, G.M., Engel, S.A., Glover, G.H., Heeger, D.J., 1996. Linear systems analysis of functional magnetic resonance imaging in human V1. J. Neurosci. 16, 4207–4221.

Branco, M.P., Gaglianese, A., Hermes, D., Saad, Z., Petridou, N., Ramsey, N.F., 2016. . Pipeline for ECoG electrode localization on brain surface: towards a one click approach, In: Proceedings of the Sixth International Brain-Computer Interface Meeting: BCI Past, Present, and Future. Asilomar Conference Center, Pacific Grove, CA USA: Verlag der Technischen Universitaet Graz, p. 154. doi:http://dx.doi.org/10.3217/978-3-85125-467-9-154.

Brookes, M.J., Gibson, A.M., Hall, S.D., Furlong, P.L., Barnes, G.R., Hillebrand, A., Singh, K.D., Holliday, I.E., Francis, S.T., Morris, P.G., 2005. GLM-beamformer method demonstrates stationary field, alpha ERD and gamma ERS co-localisation with fMRI BOLD response in visual cortex. Neuroimage 26, 302–308. http://dx.doi.org/10.1016/j.neuroimage.2005.01.050.

Chawla, D., Phillips, J., Buechel, C., Edwards, R., Friston, K.J., 1998. Speed-dependent motion-sensitive responses in V5: an fMRI study. Neuroimage 7, 86–96. http://dx.doi.org/10.1006/nimg.1997.0319.

Costagli, M., Ueno, K., Sun, P., Gardner, J.L., Wan, X., Ricciardi, E., Pietrini, P., Tanaka, K., Cheng, K., 2014. Functional signalers of changes in visual stimuli: cortical responses to increments and decrements in motion coherence. Cereb. Cortex 24, 110–118. http://dx.doi.org/10.1093/cercor/bhs294.

Dale, A.M., 1999. Optimal experimental design for event-related fMRI. Hum. Brain Mapp. 8, 109–114.

Dumoulin, S.O., Bittar, R.G., Kabani, N.J., Baker, C.L., Le Goualher, G., Bruce Pike, G., Evans, A.C., 2000. A new anatomical landmark for reliable identification of human area V5/MT: a quantitative analysis of sulcal patterning. Cereb. Cortex 10, 454–463. http://dx.doi.org/10.1093/cercor/10.5.454.

Gaglianese, A., Costagli, M., Ueno, K., Ricciardi, E., Bernardi, G., Pietrini, P., Cheng, K., 2015. The direct, not V1-mediated, functional influence between the thalamus and middle temporal complex in the human brain is modulated by the speed of visual motion. Neuroscience 284, 833–844. http://dx.doi.org/10.1016/j.neuroscience.2014.10.042.

Gaglianese, A., Harvey, B.M., Vansteensel, M.J., Dumoulin, S.O., Ramsey, N.F., Petridou, N., 2016. Separate spatial and temporal frequency tuning to visual motion in human MT 1 measured with ECoG. Hum. Brain Mapp. 38, 293–307. http://dx.doi.org/10.1002/hbm.23361, (2017).

Gagnon, L., Sakadzic, S., Lesage, F., Musacchia, J.J., Lefebvre, J., Fang, Q., Yucel, M.A., Evans, K.C., Mandeville, E.T., Cohen-Adad, J., Polimeni, J.R., Yaseen, M.A., Lo, E.H., Greve, D.N., Buxton, R.B., Dale, A.M., Devor, A., Boas, D.A., 2015. Quantifying the microvascular origin of BOLD-fMRI from first principles with two-photon microscopy and an oxygen-sensitive nanoprobe. J Neurosci. 35 (8), 3663–3675.

Gardner, J.L., Sun, P., Waggoner, R.A., Ueno, K., Tanaka, K., Cheng, K., 2005. Contrast adaptation and representation in human early visual cortex. Neuron 47, 607–620. http://dx.doi.org/10.1016/j.neuron.2005.07.016.

Goense, J., Merkle, H., Logothetis, N.K., 2012. High-resolution fMRI reveals laminar differences in neurovascular coupling between positive and negative BOLD responses. Neuron 76, 629–639. http://dx.doi.org/10.1016/j.neuron.2012.09.019.

Harvey, B.M., Vansteensel, M.J., Ferrier, C.H., Petridou, N., Zuiderbaan, W., Aarnoutse, E.J., Bleichner, M.G., Dijkerman, H.C., van Zandvoort, M.J.E., Leijten, F.S.S., Ramsey, N.F., Dumoulin, S.O., 2013. Frequency specific spatial interactions in human electrocorticography: v1 alpha oscillations reflect surround suppression. Neuroimage 65, 424–432. http://dx.doi.org/10.1016/j.neuroimage.2012.10.020.

Hermes, D., Miller, K.J., Noordmans, H.J., Vansteensel, M.J., Ramsey, N.F., 2010. Automated electrocorticographic electrode localization on individually rendered brain surfaces. J. Neurosci. Methods 185, 293–298. http://dx.doi.org/10.1016/j.jneumeth.2009.10.005.

Hermes, D., Miller, K.J., Vansteensel, M.J., Aarnoutse, E.J., Leijten, F.S.S., Ramsey, N.F., 2012. Neurophysiologic correlates of fMRI in human motor cortex. Hum. Brain Mapp. 33, 1689–1699. http://dx.doi.org/10.1002/hbm.21314.

Hirsch, S., Reichold, J., Schneider, M., Sze´kely, G., Weber, B., 2012. Topology and hemodynamics of the cortical cerebrovascular system. J. Cereb. Blood Flow. Metab. 32, 952–967.

Huk, A.C., Dougherty, R.F., Heeger, D.J., 2002. Retinotopy and functional subdivision of human areas MT and MST. J. Neurosci. 22, 7195–7205, (doi:20026661).

Huo, B.-X., Smith, J.B., Drew, P.J., 2014. Neurovascular coupling and decoupling in the cortex during voluntary locomotion. J. Neurosci. 34, 10975–10981. http://dx.doi.org/10.1523/JNEUROSCI.1369-14.2014.

Im, C.-H., Gururajan, A., Zhang, N., Chen, W., Hei, B., 2007. Spatial resolution of EEG cortical source imaging revealed by localization of retinotopic organization in human primary visual cortex. J. Neurosci. Methods 161 (1), 142–154.

Jacobs, J., Kahana, M.J., 2010. Direct brain recordings fuel advances in cognitive electrophysiology. Trends Cogn. Sci. 14 (4), 162–171.

Jacques, C., Witthoft, N., Weiner, K.S., Foster, B.L., Rangarajan, V., Hermes, D., Miller, K.J., Parvizi, J., Grill-Spector, K., 2016. Corresponding ECoG and fMRI category-selective signals in human ventral temporal cortex. Neuropsychologia 83, 14–28. http://dx.doi.org/10.1016/j.neuropsychologia.2015.07.024.

Kastner, S., O'Connor, D.H., Fukui, M.M., Fehd, H.M., Herwig, U., Pinsk, M. a, 2003. Functional imaging of the human lateral geniculate nucleus and pulvinar. J. Neurophysiol. 17, 17. http://dx.doi.org/10.1152/jn.00553.2003.

Liu, J.V., Hirano, Y., Nascimento, G.C., Stefanovic, B., Leopold, D.A., Silva, A.C., 2013. fMRI in the awake marmoset: somatosensory-evoked responses, functional connectivity, and comparison with propofol anesthesia. Neuroimage 78, 186–195.

Logothetis, N.K., Pauls, J., Augath, M., Trinath, T., Oeltermann, A., 2001. Neurophysiological investigation of the basis of the fMRI signal. Nature 412, 150–157. http://dx.doi.org/10.1038/35084005.

Lui, L.L., Bourne, J.A., Rosa, M.G.P., 2007. Spatial and temporal frequency selectivity of neurons in the middle temporal visual area of new world monkeys (Callithrix jacchus). Eur. J. Neurosci. 25, 1780–1792. http://dx.doi.org/10.1111/j.1460-9568.2007.05453.x.

Magri, C., Logothetis, N.K., Panzeri, S., 2011. Investigating static nonlinearities in neurovascular coupling. Magn. Reson. Imaging 29, 1358–1364. http://dx.doi.org/10.1016/j.mri.2011.04.017.

Magri, C., Schridde, U., Murayama, Y., Panzeri, S., Logothetis, N.K., 2012. The amplitude and timing of the BOLD signal reflects the relationship between local field potential power at different frequencies. J. Neurosci. 32, 1395–1407. http://dx.doi.org/10.1523/JNEUROSCI.3985-11.2012.

Miller, K.J., Sorensen, L.B., Ojemann, J.G., den Nijs, M., 2009. Power-law scaling in the brain surface electric potential. PLoS Comput. Biol. 5, e1000609. http://dx.doi.org/10.1371/journal.pcbi.1000609.

Mukamel, R., Gelbard, H., Arieli, A., Hasson, U., Fried, I., Malach, R., 2005. Coupling between neuronal firing, field potentials, and FMRI in human auditory cortex. Science 309, 951–954. http://dx.doi.org/10.1126/science.1110913.

Neggers, S.F.W., Hermans, E.J., Ramsey, N.F., 2008. Enhanced sensitivity with fast three-dimensional blood-oxygen-level-dependent functional MRI: comparison of SENSE-PRESTO and 2D-EPI at 3 T. NMR Biomed. 21, 663–676. http://dx.doi.org/10.1002/nbm.1235.

Niessing, J., Ebisch, B., Schmidt, K.E., Niessing, M., Singer, W., Galuske, R. a W., 2005. Hemodynamic signals correlate tightly with synchronized gamma oscillations. Science 309, 948–951. http://dx.doi.org/10.1126/science.1110948.

Norup, N., Lauritzen, M., 2001. Coupling and uncoupling of activity-dependent increases of neuronal activity and blood flow in rat somatosensory cortex. J. Physiol. 533, 773–785, doi:PHY_11382 [pii].

Ogawa, S., Lee, T.M., Kay, A.R., Tank, D.W., 1990. Brain magnetic resonance imaging with contrast dependent on blood oxygenation. Proc. Natl. Acad. Sci. USA 87, 9868–9872. http://dx.doi.org/10.1073/pnas.87.24.9868.

Ogawa, S., Tank, D.W., Menon, R., Ellermann, J.M., Kim, S.G., Merkle, H., Ugurbil, K., 1992. Intrinsic signal changes accompanying sensory stimulation: functional brain mapping with magnetic resonance imaging. Proc. Natl. Acad. Sci. USA 89, 5951–5955. http://dx.doi.org/10.1073/pnas.89.13.5951.

Onton, J., Makeig, S., 2009. High-frequency broadband modulations of electroencephalographic spectra. Front Hum. Neurosci. 3, 61. http://dx.doi.org/10.3389/neuro.09.061.2009.

Pisaro, M.A., Dhruv, N.T., Garandini, M., Benucci, A., 2013. Fast hemodynamic responses in the visual cortex of the awake mouse. J. Neurosci. 33 (46), 18343–18351.

Ramsey, N.F., Tallent, K., Van Gelderen, P., Frank, J.A., Moonen, C.T.W., Weinberger, D.R., 1996. Reproducibility of human 3D fMRI brain maps acquired during a motor task. Hum. Brain Mapp. 4, 113–121. http://dx.doi.org/10.1002/(SICI)1097-0193(1996)4:2 < 113::AID-HBM3 > 3.0.CO;2-6.

Rosa, M.J., Kilner, J., Blankenburg, F., Josephs, O., Penny, W., 2010. Estimating the transfer function from neuronal activity to BOLD using simultaneous EEG-fMRI. Neuroimage 49, 1496–1509. http://dx.doi.org/10.1016/j.neuroimage.2009.09.011.

Siero, J.C.W., Hermes, D., Hoogduin, H., Luijten, P.R., Petridou, N., Ramsey, N.F., 2013. BOLD consistently matches electrophysiology in human sensorimotor cortex at increasing movement rates: a combined 7T fMRI and ECoG study on neurovascular coupling. J. Cereb. Blood Flow. Metab. 33, 1448–1456. http://dx.doi.org/10.1038/jcbfm.2013.97.

Singh, K.D., Barnes, G.R., Hillebrand, A., Forde, E.M.E., Williams, A.L., 2002. Task-related changes in cortical synchronization are spatially coincident with the

hemodynamic response. Neuroimage 16, 103–114. http://dx.doi.org/10.1006/nimg.2001.1050.
Swettenham, J., Muthukumaraswamy, S., Singh, K., 2013. BOLD responses in human primary visual cortex are insensitive to substantial changes in neural activity. Front. Hum. Neurosci. 7, 1–11. http://dx.doi.org/10.3389/fnhum.2013.00076.
Tootell, R.B.H., Reppas, J.B., Kwong, K.K., Rosen, B.R., Belliveaul, J.W., Malach, R., 1995. Functional analysis of human MT and related visual cortical areas using magnetic resonance imaging. J. Neurosci. 15 (4), 3215–3220.
van Gelderen, P., Duyn, J.H., Ramsey, N.F., Liu, G., Moonen, C.T.W., 2012. The PRESTO technique for fMRI. Neuroimage.. http://dx.doi.org/10.1016/j.neuroimage.2012.01.017.
Vigneau-Roy, N., Bernier, M., Descoteaux, M., Whittingstall, K., 2014. Regional variations in vascular density correlate with resting-state and task-evoked blood oxygen level-dependent signal amplitude. Hum. Brain Mapp. 35 (5), 1906–1920.
Weber, B., Keller, A.L., Reichold, J., Logothetis, N.K., 2008. The microvascular system of the striate and extrastriate visual cortex of the macaque. Cereb. Cortex 18, 2318–2330.
Wells, W.M., III, Viola, P., Atsumi, H., Nakajima, S., Kikinis, R., 1996. Multi-modal volume registration by maximization of mutual information. Med. Image Anal. 1, 35–51.
Winawer, J., Kay, K.N., Foster, B.L., Rauschecker, A.M., Parvizi, J., Wandell, B.A., 2013. Asynchronous broadband signals are the principal source of the BOLD response in human visual cortex. Curr. Biol. 23, 1145–1153. http://dx.doi.org/10.1016/j.cub.2013.05.001.